

# Reversible and selective interconversion of hydrogen and carbon dioxide into formate by a semi-artificial formate hydrogenlyase mimic

Katarzyna P. Sokol,<sup>1,‡</sup> William E. Robinson,<sup>1,‡</sup> Ana R. Oliveira,<sup>2</sup> Sonia Zacarias,<sup>2</sup> Chong-Yong Lee,<sup>1</sup> Christopher Madden,<sup>1</sup> Arnau Bassegoda,<sup>3</sup> Judy Hirst,<sup>3</sup> Inês A. C. Pereira,<sup>2</sup> Erwin Reisner<sup>1,\*</sup>

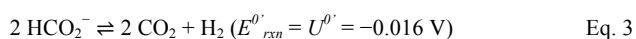
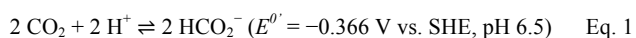
1. Department of Chemistry, University of Cambridge, Lensfield Road, Cambridge CB2 1EW, UK
2. Instituto de Tecnologia Química e Biológica António Xavier (ITQB), Universidade NOVA de Lisboa, Av. da República, 2780-157 Oeiras, Portugal
3. Medical Research Council Mitochondrial Biology Unit, University of Cambridge, The Keith Peters Building, Cambridge Biomedical Campus, Hills Road, Cambridge CB2 0XY, UK

## Supporting Information Placeholder

**ABSTRACT:** The biological formate hydrogenlyase (FHL) complex links a formate dehydrogenase (FDH) to a hydrogenase (H<sub>2</sub>ase) and produces H<sub>2</sub> and CO<sub>2</sub> from formate via mixed-acid fermentation in *Escherichia coli*. Here, we describe an electrochemical and a colloidal semi-artificial FHL system that consists of an FDH and a H<sub>2</sub>ase immobilized on conductive indium tin oxide (ITO) as an electron relay. These *in vitro* systems benefit from the efficient wiring of a highly active enzyme pair and allow for the reversible conversion of formate to H<sub>2</sub> and CO<sub>2</sub> under ambient temperature and pressure. The hybrid systems provide a template for the design of synthetic catalysts and surpass the FHL complex *in vivo* by storing and releasing H<sub>2</sub> on demand by interconverting CO<sub>2</sub>/H<sub>2</sub> and formate with minimal bias in either direction.

Semi-artificial catalytic systems combine synthetic and biological units to drive challenging reactions and provide new concepts for catalyst design.<sup>1</sup> Such solar-driven systems have already demonstrated coupling of water oxidation to the production of fuels (reduction of protons and CO<sub>2</sub>).<sup>2-5</sup> However, storage and transport of energy vectors are also important components in energy production-utilization cycles and their development will benefit from more advanced concepts and model systems.

H<sub>2</sub> is a promising fuel and its storage in formate allows for easier storage and transport; H<sub>2</sub> and formate are therefore an attractive energy vector pair. Furthermore, H<sub>2</sub> gas cleanly separates from dissolved formate, and their interconversion comes at little thermodynamic cost (Eq. 1-3).<sup>6,7</sup> However, achieving kinetic efficiency in HCO<sub>2</sub><sup>-</sup>/H<sub>2</sub> interconversion remains a synthetic challenge. Artificial systems commonly compete between decomposition of formic acid to CO and H<sub>2</sub>O (dehydration), and CO<sub>2</sub> and H<sub>2</sub> (dehydrogenation), and rely on precious metals, high temperature/pressure, organic solvents and light.<sup>8-10</sup>



FHL complexes are biological machines for HCO<sub>2</sub><sup>-</sup>/H<sub>2</sub> interconversion<sup>11</sup> that are either membrane-associated complexes composed of a multisubunit [NiFe]-H<sub>2</sub>ase coupled to a FDH,<sup>11-13</sup> or

smaller soluble complexes of an [FeFe]-H<sub>2</sub>ase and an FDH.<sup>14,15</sup> The *Escherichia coli* FHL-1 complex, composed of the membrane-bound [NiFe]-H<sub>2</sub>ase 3 (HYD-3/HycE) and FDH-H (FdhF; Figure 1a) represents a well-studied FHL, evolving H<sub>2</sub> under fermentative conditions.<sup>11,12</sup> The constituent enzymatic units of FHL-1 have been demonstrated to be reversible electrocatalysts,<sup>16-20</sup> but the complex is catalytically biased toward H<sub>2</sub> production from formate.<sup>14,15,19</sup> Interconversion of HCO<sub>2</sub><sup>-</sup>/H<sub>2</sub> has also been reported in whole-cell studies,<sup>14,20</sup> notably in sulfate-reducing bacteria in the absence of sulfate.<sup>21,22</sup> *Desulfovibrio vulgaris* Hildenborough can grow by converting formate to H<sub>2</sub>,<sup>23</sup> with formate oxidation catalyzed by a periplasmic FDH, and H<sub>2</sub> produced either via a direct pathway (periplasmic H<sub>2</sub>ase) or via transmembrane electron transfer (cytoplasmic H<sub>2</sub>ase).<sup>24</sup>

Redox biocatalysts, including H<sub>2</sub>ases and FDHs, have been coupled to other enzymatic processes via electron relays. H<sub>2</sub>ases have been connected to nitrate and fumarate reductases,<sup>25</sup> diaphorase modules,<sup>26</sup> nicotinamide reductase and alcohol dehydrogenase<sup>27</sup> via graphitic particles. Coupling a H<sub>2</sub>ase to carbon monoxide dehydrogenase efficiently catalyzed the water-gas shift reaction.<sup>28</sup> Enzymatic cascades have linked FDH with formaldehyde and alcohol dehydrogenases for methanol production.<sup>29,30</sup> However, the reversible interconversion of substrate and product has not been previously accomplished with such coupled enzymes *in vitro*.

Here, a semi-artificial FHL complex mimic is presented by rewiring FDH<sup>31,32</sup> and H<sub>2</sub>ase<sup>33</sup> from *D. vulgaris* Hildenborough into electrochemical and colloidal systems (Figure 1b,c). These systems rely on efficient electrical contact of the [W/Se]-FDH active-site via four [Fe<sub>4</sub>S<sub>4</sub>] clusters and the [NiFeSe]-H<sub>2</sub>ase active-site via three [Fe<sub>4</sub>S<sub>4</sub>] clusters with nanostructured ITO.

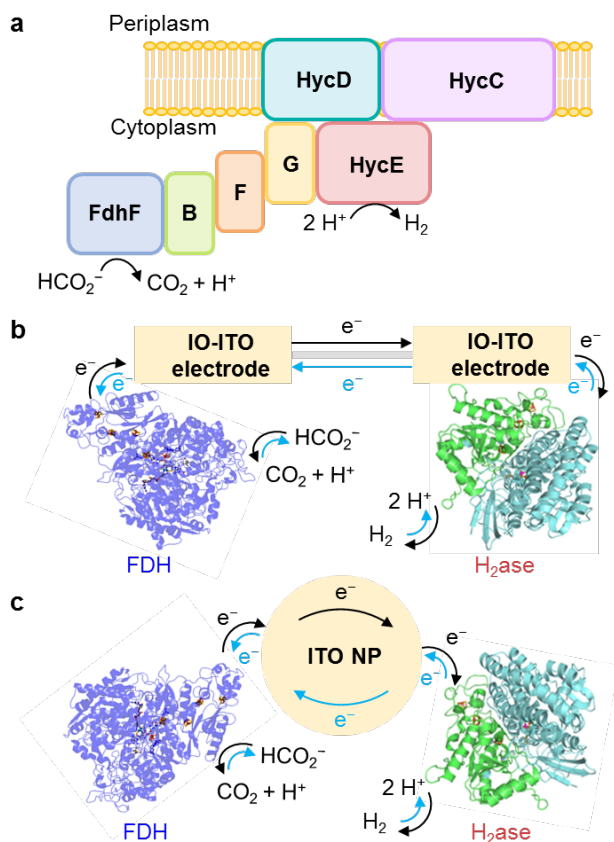


**Figure 1.** (a) Biological *E. coli* FHL-1 complex. FdhF, [Mo]-FDH; B/F/G, Fe-S cluster-containing proteins; HycE, [NiFe]-H<sub>2</sub>ase; HycD/C, membrane proteins.<sup>17</sup> (b) IO-ITO|FDH||IO-ITO|H<sub>2</sub>ase cell: IO-ITO|FDH wired to IO-ITO|H<sub>2</sub>ase electrode. (c) FDH-ITO-H<sub>2</sub>ase nanoparticle (NP) system with enzymes immobilized onto ITO NP in solution. Species size not drawn to scale.

Macro-mesoporous inverse opal (IO) ITO electrodes (20  $\mu\text{m}$  film thickness; 0.25  $\text{cm}^2$  geometrical surface area) were assembled as previously reported.<sup>34</sup> IO-ITO|FDH and IO-ITO|H<sub>2</sub>ase electrodes were prepared by drop-casting an FDH solution (2  $\mu\text{L}$ , 19  $\mu\text{M}$  with 50 mM DL-dithiothreitol, incubated for 15 min) and a H<sub>2</sub>ase solution (2  $\mu\text{L}$ , 5  $\mu\text{M}$ ), onto IO-ITO.<sup>31,34</sup> Protein film voltammetry (PFV) was recorded using a three-electrode configuration (Figure 2a and S1) in CO<sub>2</sub>/NaHCO<sub>3</sub> solution. Current densities ( $J$ ) of  $-185 \mu\text{A cm}^{-2}$  (CO<sub>2</sub> reduction to formate by FDH) and  $-450 \mu\text{A cm}^{-2}$  (H<sup>+</sup> reduction to H<sub>2</sub> by H<sub>2</sub>ase) were observed at an applied potential ( $E_{\text{app}}$ ) of  $-0.6 \text{ V}$  vs. standard hydrogen electrode (SHE). Addition of sodium formate (20 mM) to the IO-ITO|FDH system resulted in formate oxidation to CO<sub>2</sub> and  $300 \mu\text{A cm}^{-2}$  was reached at  $-0.2 \text{ V}$  vs. SHE. After purging the IO-ITO|H<sub>2</sub>ase system with H<sub>2</sub> (0.4 bar), H<sub>2</sub> oxidation to H<sup>+</sup> was observed and  $440 \mu\text{A cm}^{-2}$  was reached at  $-0.2 \text{ V}$  vs. SHE. The voltammograms cut through zero current around the formal redox potentials (Eq. 1,2), demonstrating reversible electrocatalysis for both enzymes.<sup>6,35</sup>

Multiple PFV scans of IO-ITO|FDH and IO-ITO|H<sub>2</sub>ase (Figure S2) showed minimal desorption/activity losses. Controlled-potential electrolysis (CPE) of IO-ITO|FDH and IO-ITO|H<sub>2</sub>ase was performed to measure H<sup>+</sup>/CO<sub>2</sub> reduction ( $E_{\text{app}} = -0.6 \text{ V}$ ) as well as H<sub>2</sub>/formate oxidation ( $E_{\text{app}} = -0.2 \text{ V}$ ) (Figure S3). Both electrodes retaining  $>90\%$  of the initial current after 24 h in both directions. Faradaic efficiencies ( $\eta_{\text{F}}$ ) for formate and H<sub>2</sub> production were determined to be 76 and 77%, respectively. Efficiency losses may be attributed to capacitive background current of porous IO-ITO,<sup>34</sup> undetected trapped product and a contribution from ITO/FTO degradation.<sup>36,37</sup>

The comparable formal redox potentials of H<sup>+</sup>/H<sub>2</sub> and CO<sub>2</sub>/HCO<sub>2</sub><sup>-</sup> conversion (Eq. 1-3), reversible catalysis of the individual enzymes, high and matching current densities, and good stability make this enzyme pair a promising candidate for assembling a reversible HCO<sub>2</sub><sup>-</sup>/H<sub>2</sub> interconversion system.<sup>6</sup> Thus, the IO-ITO|FDH (working electrode) was wired to the IO-ITO|H<sub>2</sub>ase (counter electrode) in a two-electrode configuration (Figure 2b). When no additional substrate was present (only buffering CO<sub>2</sub> and H<sup>+</sup>), only a non-catalytic (capacitive) current was observed. Upon addition of formate, an oxidative current was observed (formate oxidation to CO<sub>2</sub> and H<sup>+</sup> reduction to H<sub>2</sub>) at a positive applied voltage ( $U > 0 \text{ V}$ );  $250 \mu\text{A cm}^{-2}$  was reached at  $U = 0.2 \text{ V}$ . Addition of H<sub>2</sub> resulted in a reductive current (H<sub>2</sub> oxidation to H<sup>+</sup> and CO<sub>2</sub> reduction to formate) with  $-250 \mu\text{A cm}^{-2}$  obtained at  $U = -0.2 \text{ V}$ .

To achieve reversible formate/H<sub>2</sub> interconversion (Eq. 3) both formate and H<sub>2</sub> were added in addition to CO<sub>2</sub> and H<sup>+</sup>. A reversible voltammogram was observed, with zero current at approximately  $U^0$  at 0.02 V. A marginally more positive or negative voltage drives the reaction in either direction, demonstrating reversible unbiased electrocatalysis, as opposed to that demonstrated for *E. coli* FHL-1.<sup>19</sup>  $200 \mu\text{A cm}^{-2}$  and  $-200 \mu\text{A cm}^{-2}$  were reached at  $U = 0.2 \text{ V}$  and  $-0.2 \text{ V}$ , respectively. Multiple PFV scans of the IO-ITO|FDH||IO-ITO|H<sub>2</sub>ase cell (Figure S4) showed stability of the system with marginal losses. Control experiments with IO-ITO|FDH (or ITO|H<sub>2</sub>ase) wired to IO-ITO (Figure S5) gave only a small capacitive current in the presence and absence of substrates.

CPE during 2 h at  $U_{\text{app}} = 0.2 \text{ V}$  with the IO-ITO|FDH||IO-ITO|H<sub>2</sub>ase cell with formate present (Figure 2c) produced H<sub>2</sub> ( $5.84 \pm 0.88 \mu\text{mol cm}^{-2}$ ) with  $\eta_{\text{F}}$  of  $(79 \pm 11)\%$ . Similarly, CPE at  $U_{\text{app}} = -0.2 \text{ V}$  for 2 h with H<sub>2</sub> present generated formate ( $5.00 \pm 0.80 \mu\text{mol cm}^{-2}$ ) with  $\eta_{\text{F}}$  of  $(81 \pm 15)\%$ . This semi-artificial system exhibited good stability, retaining  $>95\%$  of its initial activity after 2 h in both directions. After equilibration, the cell exhibited high bidirectional stability for  $>1$  day (Figure S6). For formate oxidation ( $U_{\text{app}} = 0.2 \text{ V}$ ), H<sub>2</sub> ( $36.28 \mu\text{mol cm}^{-2}$ ) was detected with  $\eta_{\text{F}} = 72\%$ . For H<sub>2</sub> oxidation ( $U_{\text{app}} = -0.2 \text{ V}$ ), formate ( $42.80 \mu\text{mol cm}^{-2}$ ) was detected with  $\eta_{\text{F}} = 77\%$ . Similarly to the three-electrode systems, capacitive currents and FTO/ITO dissolution<sup>36,37</sup> might have decreased the product yield.

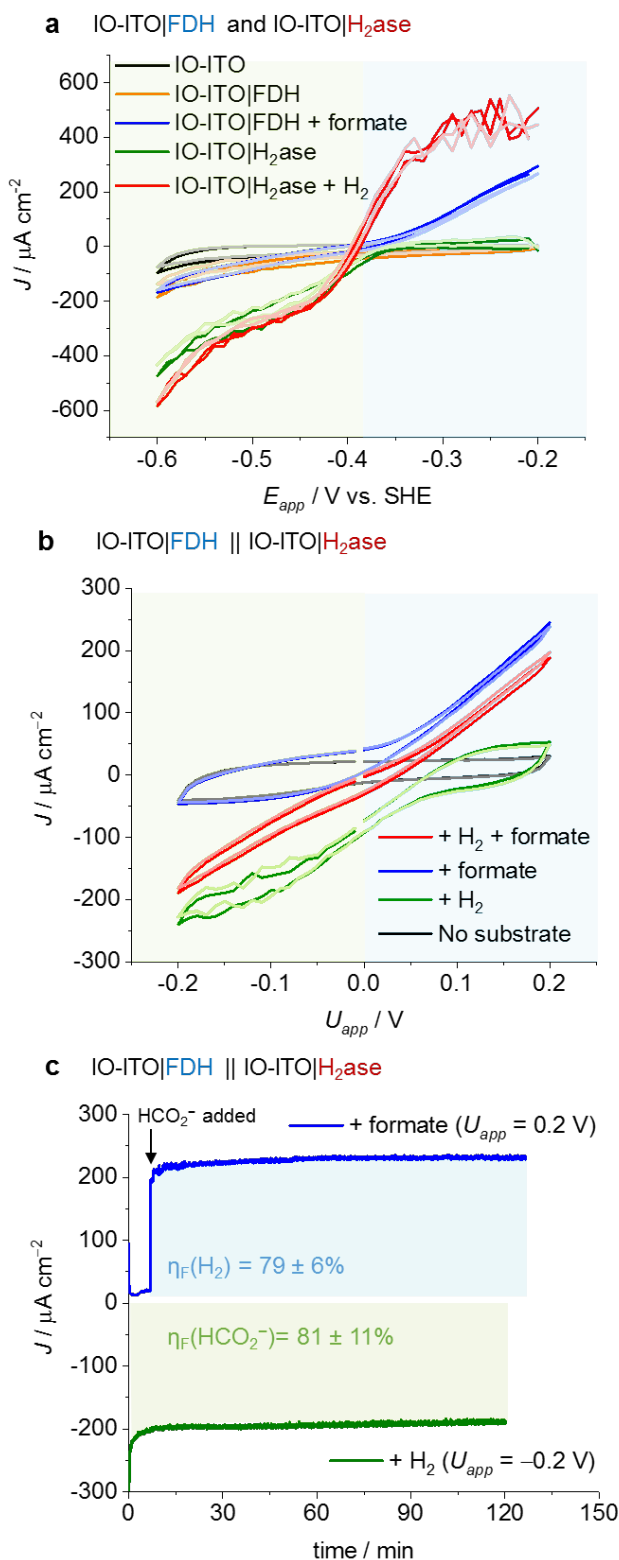


**Figure 2.** (a) Three-electrode PFV ( $v = 5 \text{ mV s}^{-1}$ , 1<sup>st</sup> and 5<sup>th</sup> scan, increasing transparency) using IO-ITO|FDH or IO-ITO|H<sub>2</sub>ase working, Ag/AgCl (KCl<sub>sat</sub>) reference, Pt counter electrode. (b) Two-electrode PFV ( $v = 5 \text{ mV s}^{-1}$ , 1<sup>st</sup> and 5<sup>th</sup> scan) of IO-ITO|FDH wired to IO-ITO|H<sub>2</sub>ase. (c) Two-electrode CPE of IO-ITO|FDH wired to IO-ITO|H<sub>2</sub>ase. Conditions: CO<sub>2</sub>/NaHCO<sub>3</sub> (100 mM), KCl (50 mM), 1 bar CO<sub>2</sub> or 0.4/0.6 bar H<sub>2</sub>/CO<sub>2</sub>, pH<sub>initial</sub> = 6.5-6.7, T = 25 °C, stirring. Substrates: formate (20 mM) and/or 0.4/0.6 bar H<sub>2</sub>/CO<sub>2</sub>.

To further investigate the system's reversibility without electrochemical wiring, FDH and H<sub>2</sub>ase were co-assembled on ITO NPs (0.3 mg mL<sup>-1</sup>) (Figure 3 and S7) dispersed in solution (see Supporting Information). Solutions of FDH (19 nM, incubated as above) and H<sub>2</sub>ase (3.4 nM) were added to the vessel, which was sealed and purged with CO<sub>2</sub>. Either formate or H<sub>2</sub> was introduced to the vessel. FDH:H<sub>2</sub>ase molar ratios (Figure S8) and total concentrations (Figure S9a,b) were screened for optimum H<sub>2</sub> evolution rate. The optimal system contained an enzyme loading of approximately 40 FDH and 7 H<sub>2</sub>ase particles per ITO NP, based on the adsorption surface area of 27 m<sup>2</sup> g<sup>-1</sup>, ~31,400 nm<sup>2</sup> per NP (assuming a 50 nm diameter sphere) and an enzyme footprint of ~100 nm<sup>2</sup>.

Upon formate addition to the FDH-ITO-H<sub>2</sub>ase system (Figure 3a), H<sub>2</sub> was produced with a rate (Figure S9c) of  $0.24 \pm 0.01 \mu\text{mol H}_2 \text{ h}^{-1}$  during the first 8 h [turnover number, TON =  $(23.0 \pm 1.5) \times 10^3$  and turnover frequency, TOF =  $6.4 \pm 0.4 \text{ s}^{-1}$  for the H<sub>2</sub>ase], after which the rate started to decrease (Table S1). Equilibrium was reached after ~72 h ( $5.82 \pm 0.24 \mu\text{mol H}_2$ , pH 6.88, T = 23 °C), in agreement with calculations ( $5.95 \mu\text{mol}$ , 2.97 mM of H<sub>2</sub>, see Supporting Information).<sup>7</sup>

In the presence of H<sub>2</sub>, the FDH-ITO-H<sub>2</sub>ase system (Figure 3b), produced formate with an initial reaction rate of  $1.33 \pm 0.01 \mu\text{mol formate h}^{-1}$  [TON =  $(15.8 \pm 5.4) \times 10^3$  and TOF =  $4.4 \pm 1.5 \text{ s}^{-1}$  for the FDH] for the first 8 h (Figure S9d). Equilibrium was reached after ~96 h ( $36.16 \pm 1.47 \mu\text{mol formate}$ , pH 6.99, T = 23 °C), consistent with calculations ( $37.11 \mu\text{mol}$ , 18.56 mM of formate).<sup>7</sup> Control experiments with no ITO NPs, omitting an enzyme or with denatured enzymes (Figure S10) showed only negligible H<sub>2</sub> and formate production (<0.2 μmol) (Table S2 and S3). Therefore, the ITO NPs act as a semi-heterogeneous electron relay facilitating electron transfer between electroactive FDH and H<sub>2</sub>ase.

In *D. vulgaris* cells, the two periplasmic enzymes exchange electrons through the type-I cytochrome *c*<sub>3</sub> (TpIc<sub>3</sub>) electron acceptor.<sup>24</sup> We therefore studied the activity of these enzymes in solution with TpIc<sub>3</sub>. A high concentration of the cytochrome (1.9 μM, 100-fold excess vs FDH) was required to achieve comparable kinetics of H<sub>2</sub> and formate production (Fig. S11a,b), revealing the superiority of co-immobilizing the two enzymes on synthetic ITO to achieve efficient electron transfer.

In summary, we have presented how semi-artificial systems consisting of FDH and H<sub>2</sub>ase from *D. vulgaris* wired to ITO can mimic the biological FHL complex. The semi-artificial FHL systems are based on a bottom-up design that employs a pair of reversible redox enzymes immobilized on conductive scaffolds to enable an overall catalytic reaction to proceed to thermodynamic equilibrium. The semi-artificial FHL concept can be deployed in either an electrochemical cell or a self-assembled colloidal suspension, providing versatility for applications in different contexts. The design concept of linking two half-reactions via a conductive scaffold also provides a blueprint to develop improved synthetic H<sub>2</sub>/formate cycling catalysts in future development.

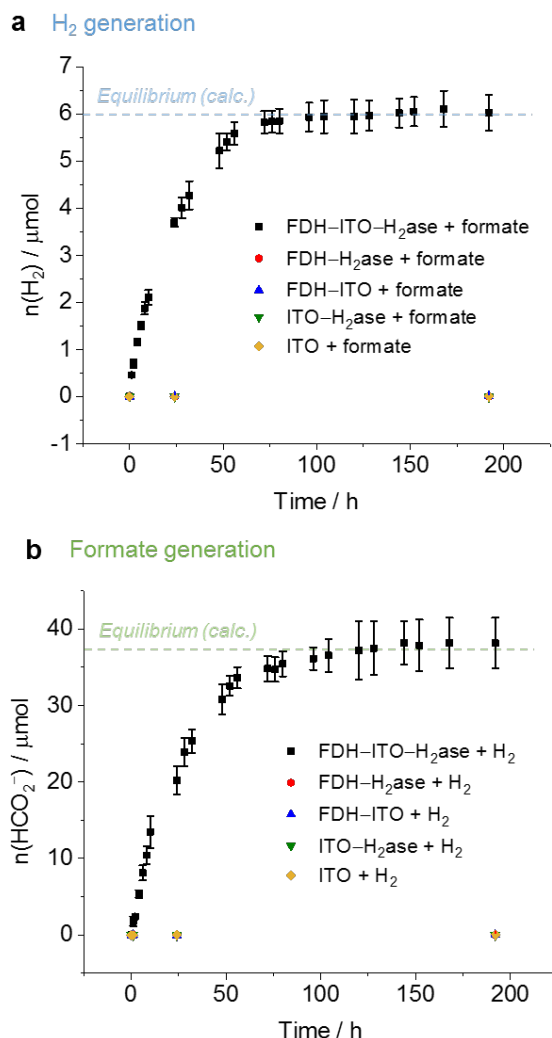


**Figure 3.** Colloidal FDH-ITO-H<sub>2</sub>ase NP system using ITO NPs (0.3 mg mL<sup>-1</sup>), FDH (19.0 nM) and H<sub>2</sub>ase (3.4 nM). (a) H<sub>2</sub> production in the presence of 10 mM formate and 1 bar CO<sub>2</sub>. V<sub>headspace</sub> = 1.72 mL. (b) Formate production in the presence of 0.4/0.6 bar H<sub>2</sub>/CO<sub>2</sub>. V<sub>solution</sub> = 2 mL. Conditions: CO<sub>2</sub>/NaHCO<sub>3</sub> (100 mM), KCl (50 mM), 1 bar CO<sub>2</sub> or 0.4/0.6 bar H<sub>2</sub>/CO<sub>2</sub>, pH<sub>initial</sub> = 6.5-6.7, T = 23 °C, stirring.

## ASSOCIATED CONTENT

### Supporting Information

Materials, experimental methods, Figures and Tables. This material is available free of charge via the ACS Publications website at <http://pubs.acs.org>.

## AUTHOR INFORMATION

### Corresponding Author

reisner@ch.cam.ac.uk

### Author Contributions

‡These authors contributed equally.

### Notes

The authors declare no competing interests.

## ACKNOWLEDGMENTS

This work was supported by ERC Consolidator Grant “MatEnSAP” (682833), BBSRC (BB/J000124/1, BB/I026367/1),

EPSRC (EP/L015978/1, EP/G037221/1, nanoDTC and a DTA studentship to K.P.S.), Marie Curie IntraEuropean Fellowship (PIEFGA-2013-625034), Fundação para a Ciência e Tecnologia (Portugal) fellowship SFRH/BD/116515/2016, grants PTDC/BIA-MIC/2723/2014, PTDC/BBB-BEP/2885/2014, R&D units UID/Multi/04551/2013 (Green-IT) and LISBOA-01-0145-FEDER-007660 (MostMicro), cofunded by FCT/MCTES and FEDER funds through COMPETE2020/POCI, and European Union’s Horizon 2020 (No 810856).

## REFERENCES

- (1) Kornienko, N.; Zhang, J. Z.; Sakimoto, K. K.; Yang, P.; Reisner, E. *Interfacing Nature’s Catalytic Machinery with Synthetic Materials for Semi-Artificial Photosynthesis*. *Nat. Nanotechnol.* **2018**, *13*, 890–899.
- (2) Woolerton, T. W.; Sheard, S.; Reisner, E.; Pierce, E.; Ragsdale, S. W.; Armstrong, F. A. *Efficient and Clean Photoreduction of CO<sub>2</sub> to CO by Enzyme-Modified TiO<sub>2</sub> Nanoparticles Using Visible Light*. *J. Am. Chem. Soc.* **2010**, *132*, 2132–2133.
- (3) Liu, C.; Gallagher, J. J.; Sakimoto, K. K.; Nichols, E. M.; Chang, C. J.; Chang, M. C. Y.; Yang, P. *Nanowire-Bacteria Hybrids for Unassisted Solar Carbon Dioxide Fixation to Value-Added Chemicals*. *Nano Lett.* **2015**, *15*, 3634–3639.
- (4) Sokol, K. P.; Robinson, W. E.; Warnan, J.; Kornienko, N.; Nowaczyk, M. M.; Ruff, A.; Zhang, J. Z.; Reisner, E. *Bias-Free Photoelectrochemical Water Splitting with Photosystem II on a Dye-Sensitized Photoanode Wired to Hydrogenase*. *Nat. Energy* **2018**, *3*, 944–951.
- (5) Brown, K. A.; Wilker, M. B.; Boehm, M.; Dukovic, G.; King, P. W. *Characterization of Photochemical Processes for H<sub>2</sub> Production by CdS Nanorod-[FeFe] Hydrogenase Complexes*. *J. Am. Chem. Soc.* **2012**, *134*, 5627–5636.
- (6) Armstrong, F. A.; Hirst, J. *Reversibility and Efficiency in Electrocatalytic Energy Conversion and Lessons from Enzymes*. *Proc. Natl. Acad. Sci. U. S. A.* **2011**, *108*, 14049–14054.
- (7) Reda, T.; Plugge, C. M.; Abram, N. J.; Hirst, J. *Reversible Interconversion of Carbon Dioxide and Formate by an Electroactive Enzyme*. *Proc. Natl. Acad. Sci. U. S. A.* **2008**, *105*, 10654–10658.
- (8) Loges, B.; Boddien, A.; Junge, H.; Beller, M. *Controlled Generation of Hydrogen from Formic Acid Amine Adducts at Room Temperature and Application in H<sub>2</sub>/O<sub>2</sub> Fuel Cells*. *Angew. Chem. Int. Ed.* **2008**, *47*, 3962–3965.
- (9) Kuehnle, M. F.; Wakerley, D. W.; Orchard, K. L.; Reisner, E. *Photocatalytic Formic Acid Conversion on CdS Nanocrystals with Controllable Selectivity for H<sub>2</sub> or CO*. *Angew. Chem. Int. Ed.* **2015**, *54*, 9627–9631.
- (10) Sordakis, K.; Tang, C.; Vogt, L. K.; Junge, H.; Dyson, P. J.; Beller, M. *Homogeneous Catalysis for Sustainable Hydrogen Storage in Formic Acid and Alcohols*. *Chem. Rev.* **2018**, *118*, 372–433.
- (11) Finney, A. J.; Sargent, F. In *Advances in Microbial Physiology*; Academic Press: London, 2019; Vol. 74.
- (12) Pinske, C. In *Advances in Microbial Physiology*; Academic Press: London, 2019; Vol. 74.
- (13) Lim, J. K.; Mayer, F.; Kang, S. G.; Muller, V. *Energy Conservation by Oxidation of Formate to Carbon Dioxide and Hydrogen via a Sodium Ion Current in a Hyperthermophilic Archaeon*. *Proc. Natl. Acad. Sci. U. S. A.* **2014**, *111*, 11497–11502.
- (14) Schuchmann, K.; Müller, V. *Direct and Reversible Hydrogenation of CO<sub>2</sub> to Formate by a Bacterial Carbon Dioxide Reductase*. *Science*. **2013**, *342*, 1382–1386.
- (15) Schwarz, F. M.; Schuchmann, K.; Müller, V. *Hydrogenation of CO<sub>2</sub> at Ambient Pressure Catalyzed by a Highly Active Thermostable Biocatalyst*. *Biotechnol. Biofuels* **2018**, *11*, 237.
- (16) Bassegoda, A.; Madden, C.; Wakerley, D. W.; Reisner, E.; Hirst, J. *Reversible Interconversion of CO<sub>2</sub> and Formate by a Molybdenum-Containing Formate Dehydrogenase*. *J. Am. Chem. Soc.* **2014**, *136*, 15473–15476.
- (17) McDowall, J. S.; Murphy, B. J.; Haumann, M.; Palmer, T.; Armstrong, F. A.; Sargent, F. *Bacterial Formate Hydrogenlyase Complex*. *Proc. Natl. Acad. Sci. U. S. A.* **2014**, *111*, E3948–E3956.



- (18) Mcdowall, J. S.; Hjersing, M. C.; Palmer, T.; Sargent, F. *Dissection and Engineering of the Escherichia Coli Formate Hydrogenlyase Complex*. *FEBS Lett.* **2015**, *589*, 3141–3147.
- (19) Pinske, C.; Sargent, F. *Exploring the Directionality of Escherichia Coli Formate Hydrogenlyase: A Membrane-Bound Enzyme Capable of Fixing Carbon Dioxide to Organic Acid*. *Microbiol. Open* **2016**, *5*, 721–737.
- (20) Roger, M.; Brown, F.; Gabrielli, W.; Sargent, F. *Efficient Hydrogen-Dependent Carbon Dioxide Reduction by Escherichia Coli*. *Curr. Biol.* **2018**, *28*, 140–145.
- (21) da Silva, S. M.; Voordouw, J.; Leitão, C.; Martins, M.; Voordouw, G.; Pereira, I. A. C. *Function of Formate Dehydrogenases in Desulfovibrio Vulgaris Hildenborough Energy Metabolism*. *Microbiology*. **2013**, *159*, 1760–1769.
- (22) Mourato, C.; Martins, M.; da Silva, S. M.; Pereira, I. A. C. *A Continuous System for Biocatalytic Hydrogenation of CO<sub>2</sub> to Formate*. *Bioresour. Technol.* **2017**, *235*, 149–156.
- (23) Martins, M.; Mourato, C.; Pereira, I. A. C. *Desulfovibrio Vulgaris Growth Coupled to Formate-Driven H<sub>2</sub> Production*. *Environ. Sci. Technol.* **2015**, *49*, 14655–14662.
- (24) Martins, M.; Mourato, C.; Morais-Silva, F. O.; Rodrigues-Pousada, C.; Voordouw, G.; Wall, J. D.; Pereira, I. A. C. *Electron Transfer Pathways of Formate-Driven H<sub>2</sub> Production in Desulfovibrio*. *Appl. Microbiol. Biotechnol.* **2016**, *100*, 8135–8146.
- (25) Vincent, K. A.; Li, X.; Blanford, C. F.; Belsey, N. A.; Weiner, J. H.; Armstrong, F. A. *Enzymatic Catalysis on Conducting Graphite Particles*. *Nat. Chem. Biol.* **2007**, *3*, 761–762.
- (26) Reeve, H. A.; Lauterbach, L.; Ash, P. A.; Lenz, O.; Vincent, K. A. *A Modular System for Regeneration of NAD Cofactors Using Graphite Particles Modified with Hydrogenase and Diaphorase Moieties*. *Chem. Commun.* **2012**, *48*, 1589–1591.
- (27) Reeve, H. A.; Lauterbach, L.; Lenz, O.; Vincent, K. A. *Enzyme-Modified Particles for Selective Biocatalytic Hydrogenation by Hydrogen-Driven NADH Recycling*. *ChemCatChem* **2015**, *7*, 3480–3487.
- (28) Lazarus, O.; Woolerton, T. W.; Parkin, A.; Lukey, M. J.; Reisner, E.; Seravalli, J.; Pierce, E.; Ragsdale, S. W.; Sargent, F.; Armstrong, F. A. *Water-Gas Shift Reaction Catalyzed by Redox Enzymes on Conducting Graphite Platelets*. *J. Am. Chem. Soc.* **2009**, *131*, 14154–14155.
- (29) Nam, D. H.; Kuk, S. K.; Choe, H.; Lee, S.; Ko, J. W.; Son, E. J.; Choi, E. G.; Kim, Y. H.; Park, C. B. *Enzymatic Photosynthesis of Formate from Carbon Dioxide Coupled with Highly Efficient Photoelectrochemical Regeneration of Nicotinamide Cofactors*. *Green Chem.* **2016**, *18*, 5989–5993.
- (30) Kuk, S. K.; Singh, R. K.; Nam, D. H.; Singh, R.; Lee, J. K.; Park, C. B. *Photoelectrochemical Reduction of Carbon Dioxide to Methanol through a Highly Efficient Enzyme Cascade*. *Angew. Chem. Int. Ed.* **2017**, *56*, 3827–3832.
- (31) Sokol, K. P.; Robinson, W. E.; Oliveira, A. R.; Warnan, J.; Nowaczyk, M. M.; Ruff, A.; Pereira, A. C.; Reisner, E. *Photoreduction of CO<sub>2</sub> with a Formate Dehydrogenase Driven by Photosystem II Using a Semi-Artificial Z-Scheme Architecture*. *J. Am. Chem. Soc.* **2018**, *140*, 16418–16422.
- (32) Miller, M.; Robinson, W. E.; Oliveira, A. R.; Heidary, N.; Kornienko, N.; Warnan, J.; Pereira, I. A. C.; Reisner, E. *Interfacing Formate Dehydrogenase with Metal Oxides for the Reversible Electrocatalysis and Solar-Driven Reduction of Carbon Dioxide*. *Angew. Chem. Int. Ed.* **2019**, *58*, 4601–4605.
- (33) Marques, M. C.; Tapia, C.; Gutiérrez-Sanz, O.; Ramos, A. R.; Keller, K. L.; Wall, J. D.; De Lacey, A. L.; Matias, P. M.; Pereira, I. A. C. *The Direct Role of Selenocysteine in [NiFeSe] Hydrogenase Maturation and Catalysis*. *Nat. Chem. Biol.* **2017**, *13*, 544–550.
- (34) Mersch, D.; Lee, C.-Y.; Zhang, J. Z.; Brinkert, K.; Fontecilla-Camps, J. C.; Rutherford, A. W.; Reisner, E. *Wiring of Photosystem II to Hydrogenase for Photoelectrochemical Water-Splitting*. *J. Am. Chem. Soc.* **2015**, *137*, 8541–8549.
- (35) Léger, C.; Bertrand, P. *Direct Electrochemistry of Redox Enzymes as a Tool for Mechanistic Studies Direct Electrochemistry of Redox Enzymes as a Tool for Mechanistic Studies*. *Chem. Rev.* **2008**, *108*, 2379–2438.
- (36) Benck, J. D.; Pinaud, B. A.; Gorlin, Y.; Jaramillo, T. F. *Substrate Selection for Fundamental Studies of Electrocatalysts and Photoelectrodes: Inert Potential Windows in Acidic, Neutral, and Basic Electrolyte*. *PLoS One* **2014**, *9*, 1–13.
- (37) Geiger, S.; Kasian, O.; Mingers, A. M.; Mayrhofer, K. J. J.; Cherevko, S. *Stability Limits of Tin-Based Electrocatalyst Supports*. *Sci. Rep.* **2017**, *7*, 3–9.

### Table of Contents artwork

